



Experimental and Numerical Investigation of Methane Combustion Combined with Biodiesel in Dual Fuel Mode

Daniel Romeo Kamta Legue^{1*}, Venant Sorel Chara-Dackou¹, Mahamat Hassane Babikir², Bali Tamegue Bernard¹, Marcel Obounou Akong¹, Paul Henri Ekobena Fouda¹

¹ Energy Laboratory, Electrical and Electronic Systems, Department of Physics, Faculty of Science, University of Yaounde 1, P.O. Box 812, Yaounde, Cameroon

² Department of Physics, University of N'djamena, P.O. Box 1117, Chad

Corresponding Author Email: campusromo@yahoo.fr

<https://doi.org/10.18280/ijht.400527>

ABSTRACT

Received: 29 September 2022

Accepted: 20 October 2022

Keywords:

biodiesel, diesel fuel, cylinder pressure, dual fuel and NO_x emission

The present work investigates experimentally and numerically the combustion of methane coupled to biodiesel and diesel in dual fuel mode. The engine used is a single-cylinder Lister-Petter_01005299_TS1 modified for bi-fuel operation with a pre-chamber in the intake to allow methane to enter with the air. For this, we use three distinct fuels, conventional D100 diesel, B100 biodiesel and methane. The first two fuels are first burned independently under the same conditions independently under the same conditions using the double Wiebe phase. The numerical results obtained of this first combustion of B100 and D100 compared to the measured results show an agreement of 2% and 1.07% respectively for biodiesel and diesel allowing the validation of the numerical code. Next, we add methane to the air during the intake phase for the previously tested D100 and B100 fuels used as a pilot fuel in order to observe the impact of methane on cylinder pressure, nitrogen oxide emissions and heat release. The combustion model used is a two-zone OD, one representing the burnt gases and the other the unburnt gases. The results showed a decrease in cylinder pressure and a large reduction in nitrogen oxide emissions of about 26.67% and about 48.76% when burning B100 biodiesel at medium load. The results also showed that the addition of methane to the air reduces the overall heat release of both fuels around TDC by 10.76% and 5.4% for biodiesel and diesel, respectively. But that in the diffusion phase, dual fuel combustion shows a higher heat release for diesel. It was also observed that peak pressures were reduced by 2.35% in the case of diesel compared to 7.45% for biodiesel.

1. INTRODUCTION

Fossil fuel reserves are exhaustible fuels, in addition to being relatively polluting and emitting greenhouse gases. Today, thermal engines consume the majority of this type of fuel, which is a major concern for this sector of activity. For years, automotive research has focused on alternative fuels that can solve the triple problem of energy savings, environmental protection and engine efficiency. As far as alternative fuels are concerned, dihydrogen is produced by the electrolysis of water. It represents a fairly energetic fuel, an alternative to fossil fuels apart from its own storage constraints. However, the storage of hydrogen and its safety index remain problematic in the field of passenger transport. In this case, natural gas appears to be a serious alternative. Natural gas is in great demand due to the large quantities that constitute the world's reserves, because of its high octane number and its ecological character [1], as is hydrogen [2]. Biogas is cheap and abundant in nature and can be easily recovered through the methanisation process. Despite these advantages, diesel is still the most useful fuel for compression-ignition engines. The most significant advantages of diesel fuel are its relatively high calorific value and its availability to meet logistical and operational requirements. The cetane number of diesel and its ignition delay are favourable for the

initiation of compression self-ignition. However, due to its unsustainable nature, particularly its combustion, which has a relatively high rate of nitrogen oxide emissions as well as particulate matter, this type of fuel is being phased out in favour of biofuels. Pending the completion of the ambitious programme of energy transition to electricity, it is necessary to find useful alternatives. These alternatives concern precisely the fuels of heavy engines, the adaptation of which to electric energy remains problematic. The combination of fuels, the dual fuel mode, is a solution whose effectiveness has been proven. Dual fuel consists of burning a primary fuel and then another fuel with high activation energy [3-5]. The work of Abo-Elfadl et al. [4] on the simulation of a dual fuel engine running on natural gas and conventional diesel has established a simulation model for the combustion of natural gas. The author shows that that depending on the proportion of natural gas added to the engine during the intake phase and the engine load, emissions are reduced compared to conventional diesel. De Robbio et al. [3] in the simplified diesel/natural gas mechanism containing 645 reactions and 155 species established a model for reducing pollutant emissions. Said et al. [6] conducted an experimental study on the effects of low loads and biogas injection pressure on the performance of the biogas-diesel engine at 1600 rpm. The results showed that a biogas injection pressure of 1 to 5.5 bar would reduce NO_x

and PM emissions by 1.94% to 77.42% respectively, as well as the cylinder pressure. The results of a study by Jia [5] showed up to 50% reduction in NOx and PM. However, the amount of carbon monoxide (CO) and unburnt hydrocarbons (HC) increases due to the poor combustion generated by the reduction of air during the intake phase. This observation requires a good calibration of the richness of the medium to obtain efficient combustion. In this sense, Aklouche et al. [7] showed that by varying the richness of the bi-fuel mixture from 0.35 to 0.7, HC and CO emissions are reduced by 77% and 58% respectively. NOx emissions were reduced by 24%. Papagiannakis and Hountalas [8] also analyzed the influence of gas flow on dual fuel combustion at different operating ranges. This analysis revealed a decrease in cylinder pressure by adding gas to the diesel combustion at medium load. Indeed, for medium operating ranges, the premixing phase takes place in lean burn, the flame develops and the cylinder pressure decreases. In lean burn, the flame does not propagate properly, which would lead to the relative increase of CO and HC emissions. This phenomenon would result in lower peak pressures and temperatures in dual fuel mode and, consequently, a reduction in nitrogen oxides [1, 5, 6, 8, 9]. With regard to alternative fuels, biofuels have been explored for decades and their performance shows that they are comparable to conventional diesel from an economic point of view. they are comparable to conventional diesel from an energy point of view, as shown by Oni et al. [2]. working on the impact of Moringa biodiesel on the combustion of compressed natural gas with hydrogen in single and dual fuel mode, the authors show that the proportion of biodiesel used as a pilot fuel reduces both nitrogen oxides, carbon monoxide and unburnt hydrocarbons. Abo-Elfadl et al. [4], in their two-zone model, simulate the combustion of an internal combustion engine. In their two-zone model, Abo-Elfadl et al. [4] simulate the combustion of a dual fuel engine fuelled by natural gas and diesel. The authors increase the volumetric efficiency of the engine by 8.7% and observe that the combustion of natural gas is slow and leads to a reduction in efficiency of about 3.5% and reduces NOx and PM emissions in dual fuel mode by about 28.6% and 86% respectively. Kamta Legue et al. [10] show that at 100% load, the peak pressure difference between Neem biodiesel and conventional diesel is 3.3%. This result was observed by several other researchers in studies of biodiesels in general, which encouraged the implementation of techniques to regulate the cylinder pressure during dual fuel combustion during biofuel combustion. The aim was to increase the longevity of the biofuel engine and reduce the resulting NOx emissions [7-12]. The solutions considered were relatively related to reducing the engine load. In addition, several authors show that the composition of diesel-biodiesel blends in appropriate proportions is one of the solutions to reduce this cylinder pressure [9-13]. The coupled reduction of pollutants in particular and of cylinder pressures when using biofuels remains a problem for diesel engines to this day. According to several researchers, dual fuel remains a reliable solution to the trade-off between energy saving, environmental preservation and engine efficiency. The use of methane as an alternative fuel has long been proven. In dual fuel mode, this requires the use of a pilot fuel capable of initiating global methane combustion. This study proposes to replace diesel by Neem-based biofuel, which has interesting predispositions, including a higher cylinder pressure than diesel combustion, a relatively high cetane number and a viscosity that decreases

proportionally with increasing engine speed. The objective of this study is to analyse the effects of burning methane as the primary fuel and Neem-based biodiesel as the pilot fuel in dual fuel mode. The implementation of this combustion mode combined with methane and Neem could improve the combustion efficiency and reduce some pollutant emissions as well as the combustion efficiency. An experimental study combined with numerical modelling could explain the effect of using methane and biodiesel on the heat release and NOx emissions of a compression-ignition engine.

2. METHODOLOGY

2.1 Methods and materials of dual fuel combustion

The combustion model used in this paper is the 0D combustion model with two zones; one zone constituting the burnt gases and the other representing the unburnt gases in the cylinder. To achieve the objective, we coupled to the 0D model, an injection system, a self-ignition, a mass fraction evolution law, a correlation for the evaluation of the heat losses and a sub-model for the evolution of the chemical species is considered under the assumption of chemical equilibrium leading to the evaluation of the polluting emissions [13-17]. The energy released during the combustion reaction is contained in the relation giving the internal energy of the system; we then have

$$dU = \delta W + \delta Q + \sum h_j dm_j \quad (1)$$

where, dU represents the change in internal energy of the system, δW represents the work supplied by the piston to the system, δQ represents the amount of heat released. The term $\sum h_j dm_j$ represents the energy due to the change in temperature. The energy due to the change in mass. In our work, the parietal heat losses are modelled using the Woschni postulate. The transformation and simplification of Eq. (1) in the burnt gas region, allows us to obtain the following system of differential equations as a function of the crank angle θ [4].

$$\begin{cases} \frac{dNO}{d\theta} = \frac{1}{\omega} \frac{6.610^{15}}{\sqrt{T}} \sqrt{[O_2]_e} [N_2]_e \exp\left(-\frac{69090}{T}\right) \\ \frac{dp}{d\theta} = \left(\frac{1}{m} \frac{dm}{d\theta} + \frac{1}{r_g} \frac{dr_g}{d\theta} + \frac{1}{T} \frac{dT}{d\theta} - \frac{1}{V} \frac{dV}{d\theta} \right) P \\ \frac{dQ}{d\theta} = \frac{dQ_{comb}}{d\theta} - \frac{dQ_p}{d\theta} = LHV \frac{dm_{fuel}}{d\theta} - \frac{dQ_p}{d\theta} \end{cases} \quad (2)$$

where, P and T represent pressure, cylinder temperature, γ the ratio of specific heats, θ the crankshaft angle, and V the cylinder volume. Where the expression for volume is governed by Eq. (2) - Eq. (8).

$$V(\theta) = \frac{\pi D^2 C}{8} \left(1 - \cos(\theta) + \lambda - \sqrt{\lambda^2 - \sin^2(\theta)} + \frac{2}{\varepsilon - 1} \right) \quad (3)$$

The term $\frac{dV}{d\theta}$ represents the change in cylinder volume V with respect to the crankshaft angle. The term $\frac{dQ}{d\theta}$ representing the total heat release rate of the system has the expression:

$$\frac{dQ}{d\theta} = \frac{dQ_{comb}}{d\theta} - \frac{dQ_p}{d\theta} = LHV \frac{dm_{fuel}}{d\theta} - \frac{dQ_p}{d\theta} \quad (4)$$

During the combustion of the dual fuel, methane is first injected into the air during the intake phase. This methane is then considered as the main fuel and the other two fuels namely Diesel D100 and B100 biodiesel are considered as the pilot fuel. The percentage β of the main fuel and the pilot fuel being regulated by the inflows of the two fuels according to the relationship below [2]:

$$\beta = \frac{\dot{m}_{pilot} LHV_{pilot}}{\dot{m}_{CH_4} LHV_{CH_4} + \dot{m}_{pilot} LHV_{pilot}} \quad (5)$$

2.2 Fuel injection and fuel evaporation

The Bernoulli equation describing the fuel injection is given by:

$$\dot{m}_{fuel} = c_d \frac{\pi d_{inj}^2}{4} n_{inj} \sqrt{\frac{2(p_{inj} - p)}{\rho_{fuel}}} \quad (6)$$

The modeling of the injection and the evolution is that described by Sombatwong et al. [18] and Huang et al. [19] and Li et al. [20]. This mass flow rate is a function of the discharge coefficient c_d injector diameter d_{inj} , the injection pressure p_{inj} and the pressure inside the cylinder p .

2.3 Auto-ignition

It has been shown by Ahmad et al. [16] have shown that the methane richness strongly conditions the dual fuel combustion. This hypothesis conditions the choice of the ignition model of the fuels. Indeed, the author shows that dual fuel combustion takes place in three main stages [21]. The auto-ignition delays as a function of the fuel richness are the following according to the correlations of Assanis and Rodriguez respectively for D100 and B100 [4, 16, 21].

$$\tau_{ID}(D100) = 2.4 p^{-1.02} \phi^{-0.2} \exp\left(\frac{2100}{T}\right) \quad (7)$$

$$\tau_{ID}(B100) = p^{-0.34} \phi^{-0.06} \exp\left(\frac{1145}{T}\right) \quad (8)$$

Dual fuel modeling incorporates the methane auto-ignition delay expressed in Ahmed et al. [16] by:

$$\tau_{ID}(CH_4) = 4.310^{-3} p^{-2.5} \phi^{-1.04} \exp\left(\frac{5000}{T}\right) \quad (9)$$

The richness ϕ being given as a function of the calorific value LHV of each fuel and the masses injected by:

$$\phi = \frac{14.5 \dot{m}_{pilot} LHV_{pilot} + 17.1 \dot{m}_{CH_4} LHV_{CH_4}}{\dot{m}_{air}} \quad (10)$$

2.4 Heat loss model

The heat loss model is given by the following equation [21-

28]:

$$\frac{dQ}{d\theta} = h_c A(\theta)(T - T_p) \frac{1}{\omega} \quad (11)$$

where, h_c is the heat exchange coefficient modeled by the Woschni correlation and $A(\theta)$ the exchange area all given respectively by the expressions:

$$h_c = 3.26 D^{-0.2} p^{0.8} T^{-0.55} \omega^{0.8} \quad (12)$$

$$A(\theta) = \pi \frac{D^2}{2} + \pi D \frac{L}{2} (\lambda + 1 - \cos \theta - \sqrt{\lambda^2 - \sin^2 \theta}) \quad (13)$$

T_p the temperature of the wall, T the temperature of the gases inside the cylinder, p the cylinder pressure, D the cylinder bore, L the piston stroke, λ the crank ratio. The term W is given by:

$$\omega = 2.28 \frac{NL}{30} + 0.00324 \frac{V_d T_a}{p_a V_a} (p - p_m) \quad (14)$$

2.5 Evolution of the fuel mass fraction

The mass fraction of the fuel was modeled according to the double phase of Wiebe and the conditions are those derived from the work of Ahmad et al. [16], giving the evolution of fuels in the combustion chamber.

$$x_b = 1 - \exp \left[-a \left(\frac{\theta - \theta_0}{\Delta \theta} \right)^{m+1} \right] \quad (15)$$

In this expression, a characterizes the Efficiency Parameter m the Form Parameter. These two parameters must be adjusted experimentally, depending on the engine and operating conditions (richness, load, injection advance...).

$$\frac{dx_b}{d\theta} = a(m+1) \left(\frac{\theta - \theta_0}{\Delta \theta} \right)^m \exp \left[-a \left(\frac{\theta - \theta_0}{\Delta \theta} \right)^{m+1} \right] \quad (16)$$

And consequently the total release of heat:

$$\frac{dQ_{comb}}{d\theta} = \frac{dQ_{combp}}{d\theta} + \frac{dQ_{combd}}{d\theta} \quad (17)$$

$$\frac{dQ_{combd}}{d\theta} = m_{fuelinj} LHV a_d (m_d + 1) \left(\frac{\theta - \theta_{0d}}{\Delta \theta_d} \right)^{m_d} \exp \left[-a_d \left(\frac{\theta - \theta_{0d}}{\Delta \theta_d} \right)^{m_d + 1} \right] \quad (18)$$

For the realization of the dual fuel, the value of the LHV varies according to the fuel that burns. In the first phase of combustion diesel or biodiesel dominates over methane and the LHV of the fuel is reduced to that of D100 or B100 depending on the pilot fuel. In the other combustion stages, the LHV of the pilot fuels and methane are taken into account. The total amount of heat released during dual fuel combustion is then expressed by Hossain et al. [17-24]:

$$Q = m_{pilot} LHV_{pilot} + m_{CH_4} LHV_{CH_4} \quad (19)$$

2.6 Model of the formation of nitrogen oxides

NO_x emissions are modeled according to the Zeldovich mechanism [13, 27-32]. It is abstracted by a set of chemical equations depending on the amount of oxygen present in the cylinder. The O₂ molecules dissociate under the effect of temperature and react with the nitrogen in the air to form nitric oxide.

$$O + N_2 \leftrightarrow NO + N \quad (20)$$

$$k_{f1} = 1.810^8 \exp\left(\frac{-38370}{T}\right)$$

$$N + O_2 \leftrightarrow NO + O \quad (21)$$

$$k_{f2} = 1.810^4 T \exp\left(\frac{-4680}{T}\right)$$

$$N + OH \leftrightarrow NO + H \quad (22)$$

$$k_{f3} = (1.8)(10^7) T \exp\left(\frac{-450}{T}\right)$$

The calculation of NO is done according to a given composition of the mixture at equilibrium. The determination of the equilibrium species involved in the combustion was done assuming that all fuels are reduced to the C-H-O system at equilibrium. The Zeldovich mechanism describes the formation of nitrogen oxides according to the equation:

$$\frac{dNO}{d\theta} = \frac{1}{\omega} \frac{(6.6)10^{15}}{\sqrt{T}} \sqrt{[O_2]_e} [N_2]_e \exp\left(\frac{-69090}{T}\right) \quad (23)$$

[O₂]_e and [N₂]_e being respectively the concentrations of oxygen and nitrogen at equilibrium. This equation is then strongly dependent on the temperature of the mixture inside the cylinder and the numerical resolution at each temperature step allows to obtain the evolution of NO formed.

3. EXPERIMENTAL SETUP

3.1 Experimental device

The experimental device consists of a single-cylinder engine with ambient air as cooling system. It is known under the name Lister Peter 0100529-TS1 [10]. It is composed of two tanks which can contain different fuels and are controlled to be injected. In the framework of the dual fuel modeling, we impose numerically that the quantity of air that enters is premixed with methane at a richness of 0.57 for the methane [16, 21] (Figure 1).

3.2 Geometric characteristics of the engine and fuels

Table 1 represents the geometrical characteristics of the engine. Table 2 represents the characteristics of the fuels useful in the numerical and experimental simulations of the D100 and B100.

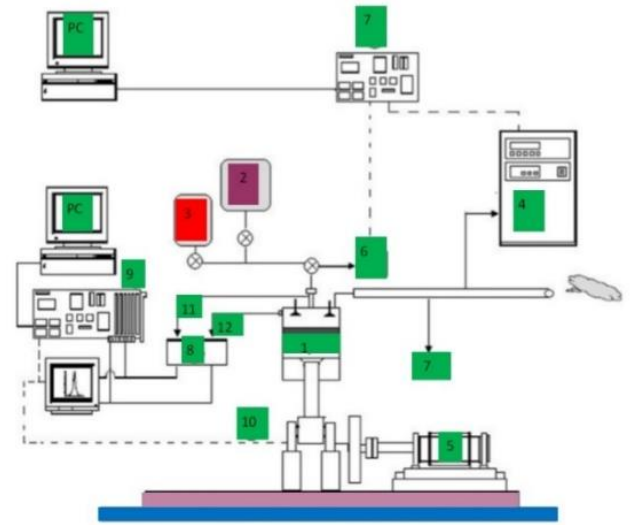


Figure 1. Expérimental set up legend (1. Diesel monocylindric motor, 2. Diesel fuel tank, 3. Alternative diesel fuel tank, 4. Exhaust gase analyser, 5. Brake drum dynamometer, 6. Matter particles analyser, 7. Low frequency acquisition system, 8. Debimeter and air flow direct, 9. High frequency acquisition system, 10. Angle encoder, 11. Injection pressure signal, 12. Cylinder pressure signal)

Table 1. Engine characteristics [9]

Lister-petter-01005299-TS1 serial		
Injection pressure	Bar	250
Piston diameter/stroke	Mm	95.3/88.9
Connecting rod length	Mm	165.3
Engine capacity	m ³	630
Compression ratio	-	18
Injection timing	degree	15° before TDC
Engine power	kW	4.5 à 1,500 trs/min

Table 2. Fuel characteristics [3]

Fuel properties	Biofuel (B100)	Diesel 100 (D100)	Methane
Density	883.3 (L)	830 (L)	0.72 (g)
Cetane Number	51.3	48	/
LHV (MJ/kg)	39.7	42.5	50
% C	0.771	0.87	0.777
% H	0.118	0.126	0.223
% O	0.109	0.004	/

4. RESULTS AND DISCUSSION

4.1 Cylinder pressure

Figures 2 and 3 present the evolution of the numerical and experimental cylinder pressures in simple combustion of biodiesel and diesel fuels. They allow to validate our numerical model from the point of view of the cylinder pressure of the two fuels compared to the experimental one.

The premixing phases are dominated by the numerical pressures compared to those measured. Indeed, at -10°V the numerical pressures of biodiesel and diesel are respectively 43.60 bars and 42.32 bars, on the other hand the respective measured values of the same fuels at -10°V have for value 42.74 bars and 41.70 bars. In this first phase of combustion,

the pressure of the biodiesel remains dominant on that of the diesel; this shows that the speed of combustion of the biodiesel as well from the experimental point of view as numerical is higher in phase of premixing compared to that of the diesel. This aspect is due to the high oxygenation of biodiesel compared to conventional diesel. The peak pressures are 74.725 bar, 72.421 bar, 73.269 bar and 71.811 bar for simulated biodiesel, simulated diesel, measured biodiesel and measured diesel respectively. That is to say an accuracy of 1.98% for biodiesel and 0.84% in the case of diesel. This discrepancy between the accuracies may be due to the ignition delay models of the two fuels. Our numerical model is in good agreement with the experimental one with a better accuracy in two zones compared to the one zone model of Kamta Legue et al. [10] which presented an accuracy of 5% under the same conditions. The numerical simulation of the two fuels can be shown in Figure 4.

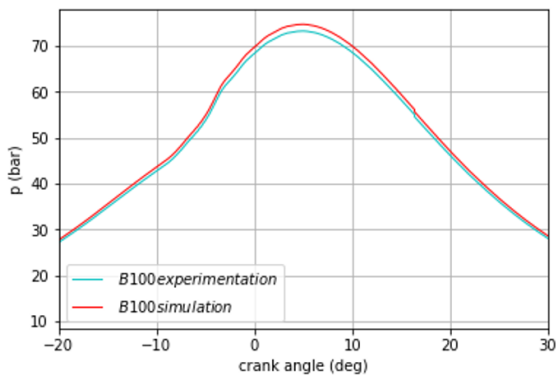


Figure 2. Comparison of simulated and experimental cylinder pressures of B100

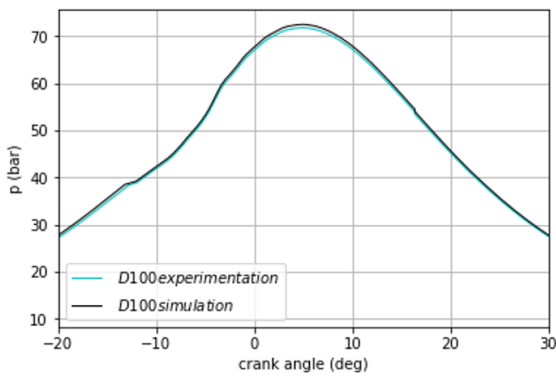


Figure 3. Comparison of simulated and experimental D100 cylinder pressures

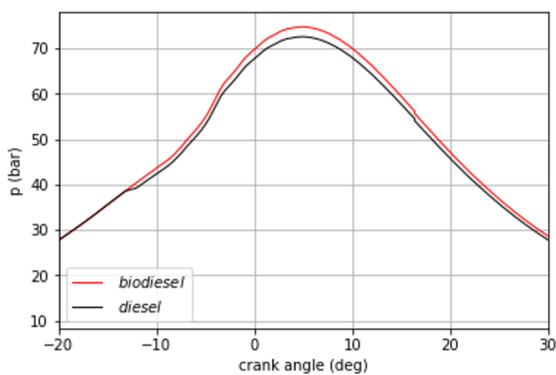


Figure 4. Comparison of simulated cylinder pressures of biodiesel with diesel

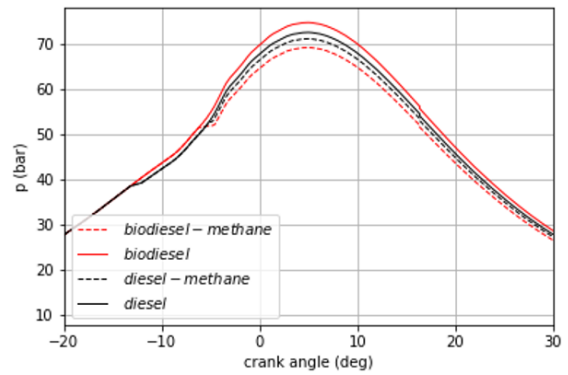


Figure 5. Comparison of fuel pressures in dual fuel mode

The comparative pressure curve shows better that during the premix combustion phase, biodiesel has a cylinder pressure difference of about 3.02% higher than diesel around -10°V before top dead center. Around top dead center, this deviation increases to about 3.17%. During the phase of the diffusion combustion in particular at 20°V we have a cylinder pressure of 47.18 bars for the combustion of biodiesel and 45.80 bars in the combustion of diesel for a difference of 3.01%. This difference is in agreement with the results of several researches such as Hossain et al. [17] and other scholars [30-36], who made the same observation on the study of the combustion and the emissions with biofuels. The difference in premix phase would reflect a relatively short auto-ignition time for biodiesel increasing the cylinder pressure because of its oxygenated character and high cetane number. Methane was added to the diesel and biodiesel fuels to observe the impact on the pressure and Figure 5 compares the cylinder pressures of the different combustion modes.

It presents a comparative evolution of the cylinder pressures of the fuels in simple mode and in dual fuel mode. The premix combustion at -10°V in dual fuel mode is marked by a similarity in simple mode because at this moment the methane present has not yet triggered its combustion, hence the similarity. On the other hand the dual fuel mode presents respectively the pressure peaks of 71.11 bars reached at 4.8°V for the diesel methane against 69.18 bars at 5.8°V for the biodiesel methane. The difference between the peak cylinder pressures in dual fuel mode and in single mode is 5.54 bars, i.e., a reduction of 8% for biodiesel and a difference of 1.4 bars, i.e., 1.84% bars for diesel. During the premix and diffusion phases the curves are closer together but around the top dead center they diverge more, this would mean that the dual fuel mode is dominant [34-37]. During the premixing phase, the dual fuel biodiesel methane presents after -10°V a deviation of 3% higher than the diesel methane.

4.2 Comparison of the mass fractions of D100 with B100

Figure 6 represents the evolution of the burned mass fractions of B100 and D100 fuels at medium load. The choice of the load being explained by Ahmed et al. [16] as the best NOx emission reduction range in dual fuel.

It can be seen that biodiesel starts to burn at 12°V before top dead center while conventional diesel will start 4°V after top dead center or 8°V before top dead center. This can be explained by the fact that the oxygenation of biodiesel leads to a better premix combustion compared to diesel. The comparison of the curves of the cylinder pressures of the two fuels showed the same observation in phase of premixing. It is

also noted that the maximums of the two curves are 0.9088 and 0.9107 respectively for diesel and biodiesel. On this difference, diesel would have more unburned hydrocarbons than biodiesel. Between -10°V and 20°V biodiesel has a large dominance of about 33.33% on the combustion process of diesel. This would also be justified by the strong oxygenated character of biodiesel leading to a dominance of the pressures and heat release of this fuel on that of diesel. This aspect gives a better energy yield but unfortunately a consequence on the higher nitrogen emissions for biodiesel according to the Zeldovich mechanism and also a lower durability of engines running on biodiesel.

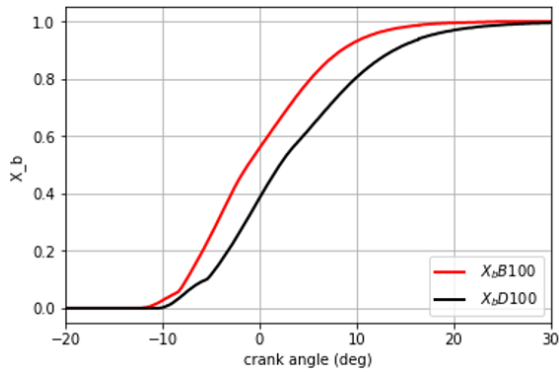


Figure 6. Evolution of the burned mass fractions B100 and D100

4.3 Heat release from fuels

The heat release curve in Figure 7 shows that, the two fuels show the same evolution and are almost confused throughout the simple combustion phase in the premix phase, but around the top dead center, biodiesel overtakes diesel. This would be due to a higher pressure rise for biodiesel than for diesel as shown in Figure 4. The peak heat release rate of biodiesel is evaluated at $36.96 \text{ J}^{\circ}\text{V}$ against $35.89 \text{ J}^{\circ}\text{V}$ for diesel, a difference of $1.07 \text{ J}^{\circ}\text{V}$. We also studied the heat release with methane as primary fuel. Figure 8 presents the heat release produced respectively by the combustion in dual-fuel mode with methane as primary fuel.

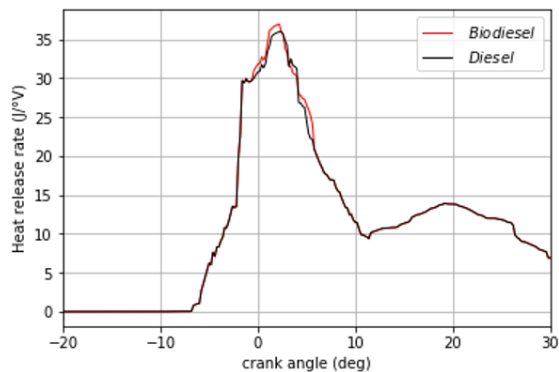


Figure 7. Biodiesel and diesel heat release

This figure shows a similarity between the combustion of diesel, biodiesel and dual-fuel. It can be seen that, during the premix combustion, the curves for dual fuel and those for diesel and biodiesel are almost identical. This can be justified by the relatively long ignition time of methane compared to biodiesel and diesel. In such a condition, the premixing phase

behaves almost like that of biodiesel and diesel fuels in single mode. On the other hand, around the top dead center and up to 7°V , diesel and biodiesel fuels supplant the dual fuel mode. Indeed, diesel methane presents a peak of $33.95 \text{ J}^{\circ}\text{V}$, i.e., a difference of $1.94 \text{ J}^{\circ}\text{V}$ compared to simple diesel. On the other hand, the biodiesel methane presents a peak of $32.98 \text{ J}^{\circ}\text{V}$ for a difference of $3.98 \text{ J}^{\circ}\text{V}$ compared to the simple diesel. This can be explained by the fact that methane combustion is relatively slower than that of diesel and biodiesel [14, 16-23] and that a good quantity of the diesel/biodiesel is compensated by methane. Nevertheless, it is noted that in dual fuel mode, the diesel/methane mixture dominates the biodiesel/methane mixture in terms of heat release with a difference of about 2.94% around the top dead center. We also note after 15°V a dominance of the diesel methane blend over all other fuels showing a late fueling of one part. This could explain the fact of the previous dominance certainly due to a dominance around the top dead center in diesel on a biodiesel mixture caused by a reduction of the calorific value of the mixture.

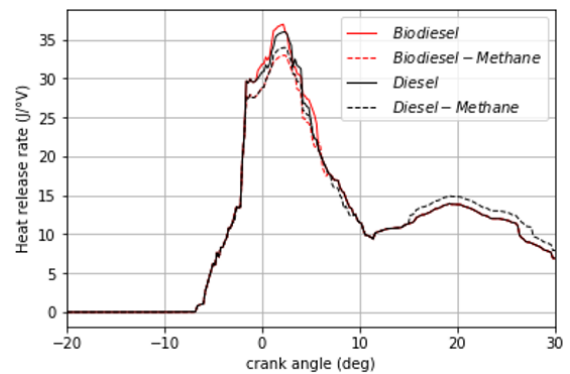


Figure 8. Comparison of the heat release rate of fuels in dual fuel mode

4.4 Nitrogen oxide emissions

The evolution of NOx in Figure 9 shows in agreement with the Zeldovich mechanism and the previous curves a dominance of nitrogen oxides during the combustion of biodiesel with a difference of 171 or about 25.71% compared to diesel emissions. This character would be justified by the high concentration of oxygen in biodiesel which favors the good progress of the combustion but also the high availability of oxygen to react with the molecules of nitrogen of the air at high temperature. Less oxygenated biodiesels will certainly make it possible to find a compromise between the energy yield and the ecological capacity factor. The modelling in dual fuel mode allowed us to present the impact of methane on NOx emissions in the presence of diesel and biodiesel as pilot fuel.

Figure 10 presents a comparative analysis of the evolution of nitrogen oxides in dual fuel mode and in single fuel mode. It shows an accentuated reduction of nitrogen oxides in the diesel methane mixture of about 48% compared to the diesel methane. This can be clearly seen on the pressure curve in dual fuel mode where the cylinder pressure of the biodiesel methane mixture shows a dominance during the premixing phase before falling back below that of the diesel methane. In general, the combustion in dual fuel mode reduces by 48.32% and 26.65% respectively in biodiesel and diesel operation. This finding has also been the subject of several studies such as that of Papagiannakis et al. [36-39]. The author reports that this decrease in NOx and state variables is due to the reduction

in the amount of oxygen intake compensated by the primary fuel input during the intake phase. The strong reduction of the biodiesel-methane dual fuel mode compared to the diesel-methane mode could be explained by the chemical properties of the biodiesel which are more important from the point of view of the cetane number and its oxygenation [40-42].

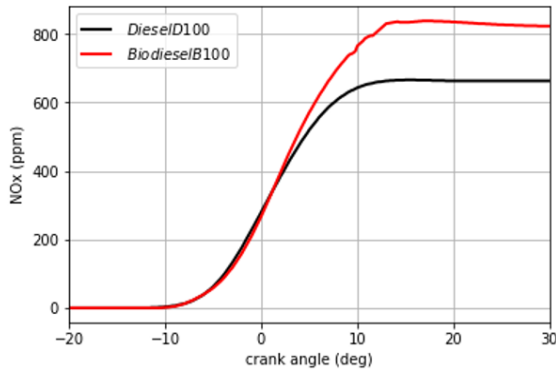


Figure 9. Comparison of nitrogen emissions from biodiesel with diesel

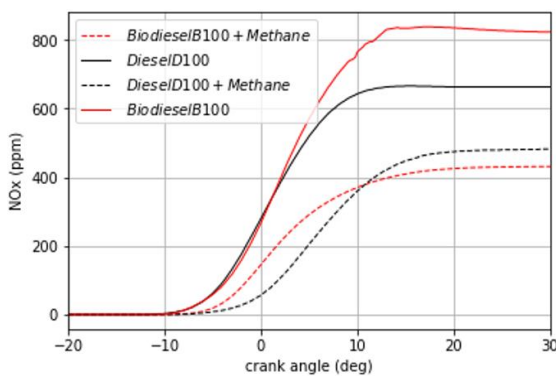


Figure 10. Comparison of nitrogen emissions of fuels in dual fuel mode

Table 3. Comparison of the different fuels

Fuel	Pic pressure	Pic heat release rate	Pic NOx (ppm)
Diesel	72.421	35.89	665
Diesel-Methane	70.9	33.95	487
Ecart diesel/diesel-methane	1.521	1.94	178
Biodiesel	74.725	36.96	836
Biodiesel-Methane	69.18	32.98	432
Ecart biodiesel/biodiesel-methane	5.545	3.98	404
Ecart diesel-biodiesel	2.304	1.07	299

Table 3 shows that biodiesel is an even better fuel when combined with methane and this can be generalized to biogas which is mostly concentrated in methane.

5. CONCLUSION

The experimentation and the simulation of the combustion of biodiesel B100 and diesel D100 have furnished the first part of this work. The numerical simulation of the dual fuel

combustion biodiesel_methane and diesel_methane has focused the attention of the second part. It was found that the combustion of biodiesel presents a faster combustion speed than that of diesel due to the high concentration of oxygen in biodiesel and its high cetane number. It shows that our two-zone 0D model has a better agreement with the diesel experimental compared to the diesel. It was also found that the addition of methane decreases the concentration of nitrogen oxides during combustion of both fuels by 26.76% for diesel and 48.32% for biodiesel as well as reducing the cylinder pressure. The reduction is more important during the combustion of diesel D100 compared to biodiesel B100. Our next work will focus on the evaluation of the 3D simulation of the dual-fuel model with methane characterization for particulate matter reduction.

REFERENCES

- [1] Rudiyanto, B., Andrianto, M., Piluharto, B., Hijriawan, M. (2022). Design-based response surface methodology in optimizing the dry washing purification process of biodiesel from waste cooking oil. *International Journal of Heat and Technology*, 40(2): 561-568, <https://doi.org/10.18280/ijht.400224>
- [2] Oni, B.A., Sanni, S.E., Ibegbu, A.J., Adujo, A.A. (2021). Experimental optimization of engine performance of a dual-fuel compression-ignition engine operating on hydrogen-compressed natural gas and Moringa biodiesel. *Energy Reports*, 7: 607-619. <https://doi.org/10.1016/j.egy.2021.01.019>
- [3] De Robbio, R., Cameretti, M.C., Tuccillo, R. (2020). Ignition and combustion modelling in a dual fuel diesel engine. *Propulsion and Power Research*, 9(2): 116-131. <https://doi.org/10.1016/j.jprr.2020.02.001>
- [4] Abo-Elfadl, S., Abdulmoez, M., M Nassib, A. (2019). Simulation modeling of a dual fuel (natural gas-diesel) engine using early direct injection technique of natural gas. *Journal of Engineering Sciences*, 47(4): 493-512. <https://doi.org/10.21608/jesaun.2019.115498>
- [5] Jia, Z. (2018). *Dual-Fuel Combustion in a Heavy-Duty Engine*. Chalmers Tekniska Hogskola (Sweden).
- [6] Said, M.A., Dalha, I.B., Karim, Z.A.A., El-Adawy, M. (2022). Influence of biogas mixing parameters on the combustion and emission characteristics of diesel RCCI engine. *Alexandria Engineering Journal*, 61(2): 1479-1497. <https://doi.org/10.1016/j.aej.2021.06.052>
- [7] Aklouche, F.Z., Loubar, K., Bentebiche, A., Awad, S., Tazerout, M. (2017). Experimental investigation of the equivalence ratio influence on combustion, performance and exhaust emissions of a dual fuel diesel engine operating on synthetic biogas fuel. *Energy Conversion and Management*, 152: 291-299. <https://doi.org/10.1016/j.enconman.2017.09.050>
- [8] Papagiannakis, R.G., Hountalas, D.T. (2004). Combustion and exhaust emission characteristics of a dual fuel compression ignition engine operated with pilot diesel fuel and natural gas. *Energy Conversion and Management*, 45(18-19): 2971-2987. <https://doi.org/10.1016/j.enconman.2004.01.013>
- [9] Mattarelli, E., Alberto Rinaldini, C., Caprioli, S., Scignoli, F. (2022). Influence of H2 enrichment for improving low load combustion stability of a Dual Fuel lightduty Diesel engine. *International Journal of Engine*

- Research, 23(5): 721-737. <https://doi.org/10.1177/14680874211051600>
- [10] Kamta Legue, D.R., Ayissi, Z.M., Babikir, M.H., Obounou, M., Ekobena Fouda, H.P. (2021). Experimental and simulation of diesel engine fueled with biodiesel with variations in heat loss model. *Energies*, 14(6): 1622. <https://doi.org/10.3390/en14061622>
- [11] Xuea J., Grift T.E., Hansen, A.C. (2011). Effect of biodiesel on engine performances and emissions. *Renewable and Sustainable Energy Reviews*, 15: 1098-1116, <https://dx.doi.org/10.1016/j.rser.2010.11.016>
- [12] Mohamed, M., Tan, C.K., Fouda, A., Gad, M.S., Abu-Elyazeed, O., Hashem, A.F. (2020). Diesel engine performance, emissions and combustion characteristics of biodiesel and its blends derived from catalytic pyrolysis of waste cooking oil. *Energies*, 13(21): 5708. <https://doi.org/10.3390/en13215708>
- [13] Bourbon, E. (2022). Clean Cities Alternative Fuel Price Report.
- [14] Abbe, C.V.N., Nzungwa, R., Danwe, R., Ayissi, Z.M., Obonou, M. (2015). A study on the 0D phenomenological model for diesel engine simulation: Application to combustion of Neem methyl ester biodiesel. *Energy Conversion and Management*, 89: 568-576. <https://doi.org/10.1016/j.enconman.2014.10.005>
- [15] Shehata, M.S. (2013). Emissions, performance and cylinder pressure of diesel engine fuelled by biodiesel fuel. *Fuel*, 112: 513-522. <https://doi.org/10.1016/j.fuel.2013.02.056>
- [16] Ahmad, Z., Kaario, O., Qiang, C., Vuorinen, V., Larmi, M. (2019). A parametric investigation of diesel/methane dual-fuel combustion progression/stages in a heavy-duty optical engine. *Applied Energy*, 251: 113191. <https://doi.org/10.1016/j.apenergy.2019.04.187>
- [17] Hossain, F.M., Nabi, M.N., Rahman, M.M., et al. (2019). Experimental investigation of diesel engine performance, combustion and emissions using a novel series of dioctyl phthalate (DOP) biofuels derived from microalgae. *Energies*, 12(10): 1964. <https://doi.org/10.3390/en12101964>
- [18] Sombatwong, P., Thaiyasuit, P., Pianthong, K. (2013). Effect of pilot fuel quantity on the performance and emission of a dual producer gas–diesel engine. *Energy Procedia*, 34: 218-227. <https://doi.org/10.1016/j.egypro.2013.06.750>
- [19] Huang, H., Lv, D., Zhu, J., Zhu, Z., Chen, Y., Pan, Y., Pan, M. (2019). Development of a new reduced diesel/natural gas mechanism for dual-fuel engine combustion and emission prediction. *Fuel*, 236: 30-42. <https://doi.org/10.1016/j.fuel.2018.08.161>
- [20] Li, Y., Li, H., Guo, H., Li, Y., Yao, M. (2017). A numerical investigation on methane combustion and emissions from a natural gas-diesel dual fuel engine using CFD model. *Applied Energy*, 205: 153-162. <https://doi.org/10.1016/j.apenergy.2017.07.071>
- [21] Schuh, S., Ramalingam, A.K., Minwegen, H., Heufer, K.A., Winter, F. (2019). Experimental investigation and benchmark study of oxidation of methane–propane–n-heptane mixtures at pressures up to 100 bar. *Energies*, 12(18): 3410. <https://doi.org/10.3390/en12183410>
- [22] Anto, S., Mukherjee, S.S., Muthappa, R., et al. (2020). Algae as green energy reserve: Technological outlook on biofuel production. *Chemosphere*, 242: 125079. <https://doi.org/10.1016/j.chemosphere.2019.125079>
- [23] Balzer, C., Kofod, M., Koot, M., Wilbrand, K. (2017). Natural gas for cleaner mobility. In *Internationaler Motorenkongress 2017*, pp. 409-427. https://doi.org/10.1007/978-3-658-17109-4_24
- [24] Bedoya, I.D., Arrieta, A.A., Cadavid, F.J. (2009). Effects of mixing system and pilot fuel quality on diesel-biogas dual fuel engine performance. *Bioresource Technology*, 100(24): 6624-6629. <https://doi.org/10.1016/j.biortech.2009.07.052>
- [25] Mansor, W.N.W., Olsen, D.B. (2016). Computational modeling of diesel and dual fuel combustion using CONVERGE CFD software. *ARPN Journal of Engineering and Applied Sciences*, 11(23): 13697-13707.
- [26] Schuh, S., Frühhaber, J., Lauer, T., Winter, F. (2019). A novel dual fuel reaction mechanism for ignition in natural gas–diesel combustion. *Energies*, 12(22): 4396. <https://doi.org/10.3390/en12224396>
- [27] Selim, M.Y. (2004). Sensitivity of dual fuel engine combustion and knocking limits to gaseous fuel composition. *Energy Conversion and Management*, 45(3): 411-425. [https://doi.org/10.1016/S0196-8904\(03\)00150-X](https://doi.org/10.1016/S0196-8904(03)00150-X)
- [28] McTaggart-Cowan, G., Mann, K., Huang, J., Singh, A., Patychuk, B., Zheng, Z.X., Munshi, S. (2015). Direct injection of natural gas at up to 600 bar in a pilot-ignited heavy-duty engine. *SAE International Journal of Engines*, 8(3): 981-996. <https://doi.org/10.4271/2015-01-0865>
- [29] Khosravi, M., Rochussen, J., Yeo, J., Kirchen, P., McTaggart-Cowan, G., Wu, N. (2016). Effect of fuelling control parameters on combustion characteristics of diesel-ignited natural gas dual-fuel combustion in an optical engine. In *Internal Combustion Engine Division Fall Technical Conference*, Greenville, South Carolina, USA, pp. V001T03A012. <https://doi.org/10.1115/ICEF2016-9399>
- [30] Heuser, B., Kremer, F., Pischinger, S., Rohs, H., Holderbaum, B., Körfer, T. (2016). An experimental investigation of dual-fuel combustion in a light duty diesel engine by in-cylinder blending of ethanol and diesel. *SAE International Journal of Engines*, 9(1): 11-25. <https://doi.org/10.4271/2015-01-1801>
- [31] Fasching, P., Sprenger, F., Preuhs, J.F., Hoffmann, G., Piock, W.F. (2017). The challenges of natural gas direct injection and its application to a natural gas-diesel dual fuel concept. In *16. Tagung Der Arbeitsprozess des Verbrennungsmotors*, pp. 461-479.
- [32] Besch, M.C., Israel, J., Thiruvengadam, A., Kappanna, H., Carder, D. (2015). Emissions characterization from different technology heavy-duty engines retrofitted for CNG/diesel dual-fuel operation. *SAE International Journal of Engines*, 8(3): 1342-1358.
- [33] Roy, M.M., Tomita, E., Kawahara, N., Harada, Y., Sakane, A. (2009). Performance and emission comparison of a supercharged dual-fuel engine fueled by producer gases with varying hydrogen content. *International Journal of Hydrogen Energy*, 34(18): 7811-7822. <https://doi.org/10.1016/j.ijhydene.2009.07.056>
- [34] Renald, C.T., Somasundaram, P. (2012). Experimental investigation on attenuation of emission with optimized LPG jet induction in a dual fuel diesel engine and prediction by ANN model. *Energy Procedia*, 14: 1427-1438. <https://doi.org/10.1016/j.egypro.2011.12.1113>
- [35] Makode, C.R., Deshmukh, M.M. (2016). Second law analysis of diesel engine by comparing different heat

transfer models. *International Journal of Engineering Research Technology*, 4(30): 2-4.

- [36] Shojae, K., Mahdavian, M. (2018). Influences of spray angle and bowl center depth on power and exhaust emissions in a dual fuel direct injection engine. *International Journal of Engine Research*, 19(6): 643-652. <https://doi.org/10.1177/1468087417727425>
- [37] Abagnale, C., Cameretti, M.C., De Simio, L., Gambino, M., Iannaccone, S., Tuccillo, R. (2014). Numerical simulation and experimental test of dual fuel operated diesel engines. *Applied Thermal Engineering*, 65(1-2): 403-417. <https://doi.org/10.1016/j.applthermaleng.2014.01.040>
- [38] Selim, M.Y. (2001). Pressure–time characteristics in diesel engine fueled with natural gas. *Renewable Energy*, 22(4): 473-489. [https://doi.org/10.1016/S0960-1481\(00\)00115-4](https://doi.org/10.1016/S0960-1481(00)00115-4)
- [39] Papagiannakis, R.G., Hountalas, D.T. (2003). Experimental investigation concerning the effect of natural gas percentage on performance and emissions of a DI dual fuel diesel engine. *Applied Thermal Engineering*, 23(3): 353-365. [https://doi.org/10.1016/S1359-4311\(02\)00187-4](https://doi.org/10.1016/S1359-4311(02)00187-4)
- [40] Lounici, M.S., Loubar, K., Tarabet, L., Balistrrou, M., Niculescu, D.C., Tazerout, M. (2014). Towards improvement of natural gas-diesel dual fuel mode: An experimental investigation on performance and exhaust emissions. *Energy*, 64: 200-211. <https://doi.org/10.1016/j.energy.2013.10.091>
- [41] Dai, X., Singh, S., Krishnan, S.R., Srinivasan, K.K. (2020). Numerical study of combustion characteristics and emissions of a diesel–methane dual-fuel engine for a wide range of injection timings. *International Journal of Engine Research*, 21(5): 781-793. <https://doi.org/10.1177/1468087418783637>
- [42] Cameretti, M.C., De Robbio, R., Tuccillo, R., Pedrozo, V., Zhao, H. (2019). Integrated CFD-experimental methodology for the study of a dual fuel heavy duty diesel engine. *SAE Technical Paper*. <https://doi.org/10.4271/2019-24-0093>

NOMENCLATURE

$A(\theta)$	area exposed to heat transfer (m^2)
B100	biodiesel
BDC	bottom Dead Center (degree)
BTDC	before TDC (degree)
D	cylinder bore (m)
D100	conventional diesel
HRR	heat Release Rate
L	stroke (m)
LHV	lower Heating Value
N	rotational speed of the engine
Q	heat transfer (kJ)
T	temperature (K)
TDC	top Dead Center (degree)
U	internal energy
V	volume (m^3)
W	work done (kJ)

Greek symbols

ε	compression ratio
θ_0	start of combustion (degree)
$\Delta\theta$	total combustion duration (degree)
θ	crank angle (degree)
λ	ratio of the rod length
ω	angular velocity (rad/s)

Subscripts

c_v	specific heat at constant volume
h_c	heat transfer coefficient ($W \cdot m^{-2} \cdot K^{-1}$)
m	masse (kg)
p	pressure (bar)
r_g	gas constant
τ_{id}	ignition delay
x_b	burnt mass fraction